Inversion of the 3-D Exponential X-ray Transform for a Semi Equatorial Band

Frédéric Noo[1], Rolf Clackdoyle[1], Jean-Marc Wagner[2] *

[1]University of Utah, USA [2]University of Liège, Belgium

1 Introduction

In this work, the reconstruction of a 3-D image from attenuated parallel-beam projections is investigated for fully 3-D data acquisition geometries.

In a partially simplified model, the measurements provided by a SPECT scanner are considered to be attenuated parallel-beam projections of the activity distribution f. They are mathematically described by the formula

$$p(\underline{\theta},\underline{s}) = \int_{-\infty}^{+\infty} dt\, f(\underline{s}+t\underline{\theta}) \exp\Big(-\int_{t}^{+\infty} dl\, \mu(\underline{s}+l\underline{\theta})\Big) \quad (1)$$

where $\underline{\theta}$ is the direction of projection defined by the orientation of the camera and the collimator holes and μ is the attenuation function. Vector $\underline{s}$ is orthogonal to $\underline{\theta}$ and is used to specify detector locations for the $p(\underline{\theta},\cdot)$ projection.

A simplication of the relation (1) between the data and the image f occurs when the activity is contained in some convex region where μ is constant. We will assume that this condition holds. In this case, the data $p(\underline{\theta},\underline{s})$ can be modified into

$$g(\underline{\theta},\underline{s}) = \int_{-\infty}^{+\infty} dt\, f(\underline{s}+t\,\underline{\theta})\, e^{\mu_0 t}, \qquad \underline{s}\cdot\underline{\theta} = 0 \quad (2)$$

where μ_0 is the value of μ in the activity region. In the literature, g is referred to as the exponential X-ray (parallel-beam) projection of f in the direction $\underline{\theta}$. The relation between p and g can be written in the form

$$g(\underline{\theta},\underline{s}) = p(\underline{\theta},\underline{s})\, m_\mu(\underline{\theta},\underline{s}) \quad (3)$$

where $m_\mu(\underline{\theta},\underline{s})$ is calculated from the attenuation map. See [1] for details. Even if the attenuation map is not known, p can be converted into g in a reasonably accurate way using the consistency conditions for the exponential X-ray transform [2].

The set of directions $\underline{\theta}$ for which p is measured defines the data acquisition geometry. We use Ω to denote this set. By definition, Ω is a subset of the unit sphere. The most common set Ω encountered in SPECT imaging is the great circle (360° scan) or half great circle (180° scan) of directions orthogonal to the patient bed. However, fully 3-D geometries are also possible, such as the RSH-SPECT scanner [3].

Image reconstruction from exponential X-ray projections on a great circle has been widely studied over the last twenty years and is now well-understood, especially thanks to the significant work of Tretiak and Metz [4] and Pan and Metz [5, 6]. In fully 3-D geometries, the situation is very different. To our knowledge, only three works concerning exact fully 3-D reconstruction from exponential X-ray projections have been published [7, 8, 9]. The most general of these assumes that the set Ω is a union of great circles.

Currently, the class of data sets for which a closed-form inversion formula of the imaging equation (2) exists is unknown. It is not even known what conditions a data set must satisfy to be complete. The 3-D reconstruction theory for X-ray projections ($\mu = 0$) [10, 11] is not easily modified to handle exponential X-ray projections.

We have derived a closed-form inversion formula for the 3-D exponential X-ray transform which is valid for any data set Ω made up of half great circles. A basic example of such a set is the half equatorial band illustrated in figure 1a; our presentation concentrates on this example.

Our results generalize all previously published results on the exponential X-ray transform[1]. They constitute one

*This work was partially supported by the National Institutes of Health, grant number R01 HL55610. The work of F. Noo was partially supported by Marconi Medical Systems.

[1]A parallel submission to this conference by Wagner, Noo and

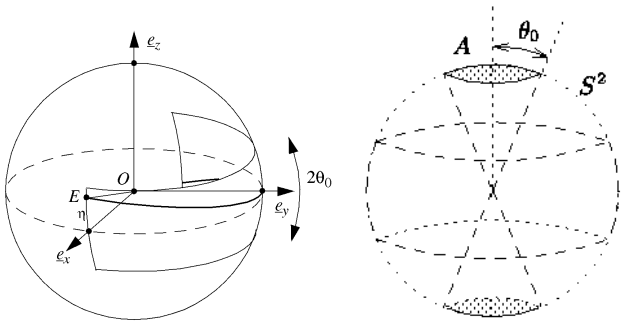

Figure 1: (a-left) Illustration of the half equatorial band (b-right) Description of the set A.

step further towards a full understanding of this transform which is an important mathematical tool in SPECT imaging and in Intensity Modulated Radiation Therapy (see [12] for more details on this latter application).

The basic idea is to combine a recent result on inversion of 180° scans [13] with the TTR concept of Ra *et al.* [14].

2 A half great circle

Let $\mathcal{C}(\underline{n}, E)$ be the right-oriented half great circle which starts at E and is orthogonal to the unit vector $\underline{n}$ on the unit sphere. See figure 1a. Let $\underline{a} = \underline{OE}$ where O is the center of the sphere and let $\underline{b} = \underline{n} \times \underline{a}$. From the results in [9] and [13], it can be shown that f satisfies the following integral equation

$$f(\underline{x}) = f_0(\underline{x}, \underline{n}, E) + w(\underline{x}, \underline{n}, E) * f(\underline{x}) \tag{4}$$

where $f_0(\underline{x}, \underline{n}, E)$ and $w(\underline{x}, \underline{n}, E)$ are defined as follows. The function $f_0(\underline{x}, \underline{n}, E)$ is obtained by filtered backprojection (FBP) of the projections on $\mathcal{C}(\underline{n}, E)$:

$$f_0(\underline{x}, \underline{n}, E) = \int_{\mathcal{C}(\underline{n}, E)} d\underline{\theta}\; e^{-\mu_0\, \underline{x}\cdot\underline{\theta}}\; g^F\Big(\underline{\theta}, \underline{x} - (\underline{x}\cdot\underline{\theta})\,\underline{\theta}\Big) \tag{5}$$

with

$$g^F(\underline{\theta}, \underline{s}) = \int_{\underline{s}'\cdot\underline{\theta}=0} d\underline{s}'\, g(\underline{\theta}, \underline{s} - \underline{s}')\, \delta(\underline{s}'\cdot\underline{n})\, k_\mu\Big(\underline{s}'\cdot(\underline{n}\times\underline{\theta})\Big) \tag{6}$$

Clackdoyle addresses geometries consisting of a union of circles on the sphere. This is a distinct class of geometries.

where k_μ is the notch filter used in the FBP formula of Tretiak and Metz for the 2-D exponential Radon transform [4], i.e.

$$k_\mu(r) = 1/2 \int_{|\nu|>\mu_0/2\pi} d\nu\, |\nu|\, e^{j2\pi r\nu}\,. \tag{7}$$

The convolution kernel $w(\underline{x}, \underline{n}, E) = \delta(\underline{x}\cdot\underline{n})\, \hat{w}(\underline{x}\cdot\underline{a}, \underline{x}\cdot\underline{b})$ where δ is the 1D Dirac function and

$$\hat{w}(u,v) = \frac{\sinh\mu_0 v}{\pi v}\, q(u) + \frac{\overline{\mu}_0}{\pi u}\Big\{\frac{2\sinh\mu_0 v}{\mu_0 v} - \frac{\sinh\mu_0(v+iu)}{\mu_0(v+iu)} - \frac{\sinh\mu_0(v-iu)}{\mu_0(v-iu)}\Big\} \tag{8}$$

In the above definition,

$$q(u) = \int_{\mathbb{R}} d\sigma\, i\,\mathrm{sign}(\sigma)\, e^{i2\pi u\sigma} \tag{9}$$

is the convolution kernel of the Hilbert transform. Note that $w(\underline{x}, \underline{n}, E)$ is an odd function in $\underline{x}$, i.e $w(-\underline{x}, \underline{n}, E) = -w(\underline{x}, \underline{n}, E)$.

Basically, for exponential projections $g(\underline{\theta}, \underline{s})$ measured on the (360°) great circle $\mathcal{C}(\underline{n}, E) \cap \mathcal{C}(\underline{n}, -E)$ the Tretiak and Metz FBP gives an accurate reconstruction f. However, on the (180°) half circle $\underline{\theta} \in \mathcal{C}(\underline{n}, E)$, the reconstruction gives an incorrect f_0. The images f_0 and f are linked by w according to equation (4).

3 An equatorial band

The discussion is now focussed on the half equatorial band of figure 1a. Let A be the set of unit vectors corresponding to all the half great circles in Ω. See figure 1b. For each vector $\underline{n}$, the starting point of the half great circle is at $\underline{OE} = \cos\eta\, \underline{e}_x + \sin\eta\, \underline{e}_z$ with

$$\tan\eta = -\,\underline{n}\cdot\underline{e}_x / \underline{n}\cdot\underline{e}_z\,. \tag{10}$$

For each half great circle in Ω, an integral equation similar to (4) can be written. Integrating equation (4) over all $\underline{n} \in A$, one obtains an integral equation for f which involves all the data from Ω:

$$f(\underline{x}) = f_0(\underline{x}) + W(\underline{x}) * f(\underline{x}) \tag{11}$$

with

$$f_0(\underline{x}) = c \int_A d\underline{n}\, f_0(\underline{x}, \underline{n}, E)\,, \tag{12}$$

and

$$W(\underline{x}) = c \int_A d\underline{n}\, w(\underline{x}, \underline{n}, E)\,. \tag{13}$$

In these equations, c is a normalization constant:

$$c = 1/\int_A d\underline{n} = 2\pi\,(1 - \cos\theta_0) \tag{14}$$

where θ_0 is the half aperture of the band.

Using the same argument as in [9], it can be shown that $f_0(\underline{x})$ can be calculated in a fully 3-D FBP way. The expression is

$$f_0(\underline{x}) = \int_\Omega d\underline{\theta}\; e^{-\mu_0\, \underline{x}\cdot\underline{\theta}}\, g^F\big(\underline{\theta}, \underline{x} - (\underline{x}\cdot\underline{\theta})\,\underline{\theta}\big) \tag{15}$$

where $g^F(\underline{\theta}, \underline{s})$ is obtained from $g(\underline{\theta}, \underline{s})$ by 2-D convolution:

$$g^F(\underline{\theta}, \underline{s}) = \int_{\underline{s}'\cdot\underline{\theta}=0} d\underline{s}'\, g(\underline{\theta}, \underline{s} - \underline{s}')\, h_\mu(\underline{\theta}, \underline{s}')\,. \tag{16}$$

The convolution filter h_μ is given by

$$h_\mu(\underline{\theta}, \underline{s}) = \begin{cases} 2\,c\,\dfrac{k_\mu(||\underline{s}||)}{||\underline{s}||} & \text{if} \quad \underline{\theta} \times \dfrac{\underline{s}}{||\underline{s}||} \in A \\ \\ 0 & \text{otherwise} \end{cases} \tag{17}$$

As readily observed from its definition, the filter h_μ is a generalized function with singularities at $\underline{s} = 0$. The implementation of equation (16) therefore requires the use of some regularization technique. For an accurate computation of $g^F(\underline{\theta}, \underline{s})$ from samples of $g(\underline{\theta}, \underline{s})$ on a Cartesian grid, we recommend the implementation of (16) in the Fourier domain with some apodizing frequency window, such as the Hanning window. Such an implementation requires the knowledge of the Fourier transform of the filter h_μ. It is shown in [9] that this transform is

$$\begin{aligned} H_\mu(\underline{\theta}, \underline{\nu}) = &\int_{\underline{s}\cdot\underline{\theta}=0} d\underline{s}\, e^{-j2\pi\underline{s}\cdot\underline{\nu}}\, h_\mu(\underline{\theta}, \underline{s}) \\ = &\frac{c}{2}\int_{\mathcal{C}_\mu(\underline{\theta})\cap A} d\underline{n}\, w(\underline{n})\,|\underline{\nu}\cdot(\underline{n}\times\underline{\theta})|\,, \qquad \underline{\nu}\cdot\underline{\theta} = 0 \end{aligned} \tag{18}$$

where $\mathcal{C}_\mu(\underline{\theta})$ is a subset of the great circle $\mathcal{C}(\underline{\theta})$ of unit vectors orthogonal to $\underline{\theta}$:

$$\mathcal{C}_\mu(\underline{\theta}) = \mathcal{C}(\underline{\theta}) \setminus \big\{\underline{n} \in \mathcal{C}(\underline{\theta}) \;:\; |\underline{\nu}\cdot(\underline{n}\times\underline{\theta})| < \mu_0/2\pi\big\}\,. \tag{19}$$

Note, in particular, that $\mathcal{C}_\mu(\underline{\theta})$ is empty when $||\underline{\nu}|| < \mu_0/2\pi$ because $|\underline{\nu}\cdot(\underline{n}\times\underline{\theta})| < \mu_0/2\pi$ for any $\underline{n}$ in this case. Therefore,

$$H_\mu(\underline{\theta}, \underline{\nu}) = 0 \quad \text{if} \quad ||\underline{\nu}|| < \mu_0/2\pi. \tag{20}$$

4 Solution of the integral equation

In this section, we show that the integral equation (11) admits a unique solution which can be expressed in the form of a Neumann series. First, note that the kernel $W(\underline{x})$ (equation (13)) is an odd function, i.e. $W(-\underline{x}) = -W(\underline{x})$ because $w(-\underline{x}, \underline{n}, E) = -w(\underline{x}, \underline{n}, E)$.

Let R be some radius such that $f(\underline{x}) = 0$ for $|\underline{x}| > R$ and let

$$\chi(\underline{x}) = \begin{cases} 1 & \text{if } |\underline{x}| < R \\ 0 & \text{otherwise} \end{cases} \tag{21}$$

In practice R is always finite since f is physically restricted to a finite region. Using χ, the integral equation (11) can be rewritten in the form

$$f = \chi\, f_0 + \chi\,(W * f) = \chi\, f_0 + K\, f \tag{22}$$

where K is an operator such that $K\,f = \chi(W * f)$. Since W is odd, we note that K is skew-symmetric.

Using the same arguments as those developed in [13], one can show that K is bounded. Let $\gamma = 1/(1 + ||K||^2)$. We introduce a modified operator $\hat{K} = (1-\gamma)\,I + \gamma\,K$ where I is the identity operator and rewrite (22) in the form

$$f = \gamma\,\chi\, f_0 + \hat{K}\, f\,. \tag{23}$$

By definition, $||\hat{K}|| < 1$. Therefore, the integral equation (23) admits a unique solution

$$f = \sum_{l=0}^{\infty} \hat{K}^l\, \chi\, f_0\,. \tag{24}$$

See [15] for mathematical details.

The reconstruction of f from formula (24) can be implemented in the following way:

- Step 1: Compute $f_0 = \chi\, f_0$ from the available projections g. See formula (15).
- Step 2: Compute $f_n = \hat{K} f_{n-1}$ for $n = 1, \ldots, N$
- Step 3: Compute $f_N \simeq \gamma \sum_{n=0}^{N} f_n\,.$

The function f_N represents the reconstructed image. The accuracy $||f_N - f||$ of the reconstruction depends on $||K||$. In the absence of noise, the smaller $||K||$, the smaller $||\hat{K}||$ and thus the smaller the number of terms N required for a given accuracy because the series converges faster.

References

[1] A. Markoe, "Fourier inversion of the attenuated X-ray transform", *SIAM J. Math. Anal.*, Vol. 15(4), 718-722, 1984.

[2] C. Mennessier, F. Noo, R. Clack, G. Bal and L. Desbat, "Attenuation correction in SPECT using consistency conditions for the exponential ray transform", *Phys. Med. Biol.*, Vol 44, 2483-2510, 1999.

[3] R. Clack, P. E. Christian, M. Defrise and A. E. Welch, "Image reconstruction for a novel SPECT system with rotating slant-hole collimators". *In Conf. Rec. 1995 IEEE Med. Imag.* Conf., 1948-1952, 1996.

[4] O. Tretiak and C. Metz, "The exponential Radon transform", *SIAM J. Appl. Math.*, Vol. 39(2), 341-354, 1980.

[5] C. E. Metz and X. Pan, "A unified analysis of exact methods of inverting the 2D exponential Radon transform, with implications for Noise Control in SPECT", *IEEE Trans. Med. Imag.*,vol. 14(4), 643-658, 1995.

[6] X. Pan and C. E. Metz, "Analysis of noise properties of a class of exact methods of inverting the 2D exponential Radon transform", *IEEE Trans. Med. Imag.*, vol. 14(4), 659-668, 1995.

[7] I. A. Hazou, "Inversion of the exponential X-ray transform. I: Analysis", *Math. Methods in the Applied Sciences*, Vol. 10(10), 561-574, 1988.

[8] Y. Weng, G. L. Zeng and G. T. Gullberg, "Filtered backprojection algorithms for attenuated parallel and cone-beam projections sampled on a sphere", *in Three-dimensional Image Reconstruction in Radiation and Nuclear Medicine*, ed. P.Grangeat and J.-L. Amans (Dordrecht: Kluwer), 19-34, 1996.

[9] J.-M. Wagner and F. Noo, "Three-dimensional image reconstruction from exponential parallel-beam projections", *IEEE Transactions on Nuclear Sciences*, (to appear) June 2001.

[10] S. S. Orlov, "Theory of three dimensional reconstruction. 1. Conditions of a complete set of projections.", *Sov. Phys.-Crystallogr.*, Vol. 20, 312-314, 1975.

[11] M. Defrise, D. W. Townsend and R. Clack, "Three-dimensional image reconstruction from complete projections", *Phys. Med. Biol.*, Vol. 34(5), 573-587, 1989.

[12] M. Braunstein and R. Y. Levine, "Optimum beam configurations in tomographic intensity modulated radiation therapy", *Phys. Med. Biol.*, Vol. 45, 305-328, 2000.

[13] F. Noo and J.-M. Wagner, "Image reconstruction in 2D SPECT with 180-degree acquisition," *submitted to Inverse Problems.*

[14] J. B. Ra, C. B. Lim, Z. H. Cho, S. K. Hilal and J. Correll "A true three-dimensional reconstruction algorithm for the spherical positron emission tomograph", *Phys. Med. Biol.*, Vol. 27, 37-50, 1982.

[15] N. I. Akhiezer and I. M. Glazman, *Theory of linear operators in Hilbert space. Volume I*, Pitman Advanced Publishing Program (Boston. London. Melbourne.), 1981.